

Research Article

Edible Bird's Nest Effectively Attenuates Atherosclerosis through Modulation of Cholesterol Metabolism via Activation of PPAR γ /LXR α Signaling Pathway *In Vivo*

Nurul Nadiah Mohamad Nasir ¹, Ramlah Mohamad Ibrahim ², Rozi Mahmud ³,
Nor Asma Ab Razak ¹, Norsharina Ismail ¹, Kim Wei Chan ¹,
and Md Zuki Abu Bakar ^{1,4}

¹Natural Medicines and Products Research Laboratory, Institute of Bioscience, Universiti Putra Malaysia, 43400 Serdang, Malaysia

²Jeffrey Cheah School of Medicine and Health Sciences, Monash University Malaysia, 47500 Petaling Jaya, Malaysia

³Department of Radiology, Faculty of Medicine and Health Sciences, Universiti Putra Malaysia, 43400 Serdang, Malaysia

⁴Department of Veterinary Pre-Clinical Science, Faculty of Veterinary Medicine, Universiti Putra Malaysia, 43400 Serdang, Malaysia

Correspondence should be addressed to Md Zuki Abu Bakar; zuki@upm.edu.my

Received 15 March 2023; Revised 3 August 2023; Accepted 30 August 2023; Published 25 September 2023

Academic Editor: Akhilesh K. Verma

Copyright © 2023 Nurul Nadiah Mohamad Nasir et al. This is an open access article distributed under the Creative Commons Attribution License, which permits unrestricted use, distribution, and reproduction in any medium, provided the original work is properly cited.

Atherosclerosis is the underlying cause of the majority of cardiovascular diseases (CVDs) due to high-cholesterol deposition in the aorta, resulting in hardening and narrowing of blood vessels and subsequently leading to an obstructed blood flow. There are few previous publications showing the preventive effects of edible bird's nest (EBN) on CVD, but the study on cholesterol homeostasis related to atherosclerosis is limited. In this study, we have determined the mechanisms by which EBN modulates cholesterol metabolism by identifying genes and biomarkers. Male New Zealand white rabbits were fed either a high-fat high-cholesterol (HFC) diet or a HFC diet supplemented with EBN (500 mg/kg b.w/day) for 12 weeks. For comparison purposes, a group of rabbits receiving a HFC diet was supplemented with simvastatin (10 mg/kg b.w/day) as a standard drug treatment for hypercholesterolemia. EBN supplementation significantly improved lipid and coagulation profiles, reduced hepatosteatosis, and stabilized atherosclerotic plaque formation in hypercholesterolemic rabbits. Cholesterol accumulation in liver and aorta tissues, as well as hepatic HMGCR levels, was reduced in the hypercholesterolemic rabbits supplemented with EBN. Gene expression analysis showed that EBN induced many genes related to cholesterol uptake (LDLR, LOX-1, and CD36), cholesterol efflux (ABCA1, LCAT, and CYP7A1), and cholesterol-sensing signaling (LXR α and PPAR γ). In conclusion, our studies suggest that EBN supplementation could be an effective food product for the treatment or prevention of atherosclerosis by regulating cholesterol metabolism.

1. Introduction

Hypercholesterolemia condition leads to pathogenic accumulation of low-density lipoprotein cholesterol (LDL-c) in blood vessels, fatty streak initiation, and atherosclerotic plaque formation, which are highly associated with the development of cardiovascular diseases (CVDs) [1]. The maintenance of hepatic cholesterol homeostasis is very

important which involves biosynthesis by hydroxy-3-methylglutaryl coenzyme A reductase (HMGCR), uptake by low-density lipoprotein receptors (LDLRs), lipoprotein release into the circulation, storage via esterification, and excretion as bile acids [2]. Disturbances in hepatic cholesterol homeostasis may also result in non-alcoholic fatty liver disease (NAFLD), which is highly associated with the pathogenesis of atherosclerosis.

The hallmark of atherosclerosis in the vascular wall happens when the oxidized LDL (oxLDL) is taken up by macrophages via scavenger receptors such as lectin-like oxidized LDL receptor-1 (LOX-1) and cell differentiation 36 (CD36) and subsequently transformed into foam cells [3, 4]. The imbalanced cholesterol uptake and efflux result in increased macrophage cholesterol levels, leading to the massive production of foam cells and the initiation of the fatty streak in the aorta [5]. Reverse cholesterol transport (RCT) is the primary pathway for cholesterol efflux in order to maintain cellular cholesterol homeostasis. In RCT, activation of transcription factors, liver X receptor alpha (LXR α) and peroxisome proliferator-activated receptor gamma (PPAR γ), has been shown to reduce the production of macrophage foam cells and the progression of fatty streaks in the subendothelial space of the vascular wall via regulation of the LXR-dependent ATP-binding cassette (ABC) pathway [5, 6].

The PPAR γ /LXR α signaling pathway upregulates the ABC subfamily A member 1 (ABCA1) expression, enabling cholesterol efflux in macrophages [7]. This leads to the production of cholesterol ester via lecithin-cholesterol acyltransferase (LCAT), which transports intracellular cholesterol to the liver as high-density lipoprotein (HDL). Low-density lipoprotein receptor (LDLR) is responsible for taking up HDL in the liver, and the cholesterol will be excreted as bile acids through cholesterol 7-hydroxylase (CYP7A1) via the activation of LXR α [8]. Inhibiting cholesterol uptake and promoting cholesterol efflux offer a therapeutic alternative for atherogenesis.

Statins are widely used to reduce the risk of atherosclerosis and NAFLD, but prolonged use can lead to side effects such as liver injury, muscle toxicity, and acute renal failure [9]. Edible bird's nest (EBN) is a natural food supplement with cardioprotective properties, modulating serum lipid profiles, coagulation status, cholesterol metabolism, and insulin sensitivity, thereby potentially aiding antiatherogenic therapeutic development [10–12]. Therefore, the aim of this paper was to determine whether the EBN possess putative serum cholesterol-lowering and antiatherogenic effects in comparison to simvastatin (a lipid-lowering drug) in diet-induced hypercholesterolemia in New Zealand white rabbits. In addition, the effects of EBN on cholesterol metabolism were assessed at molecular levels in order to elucidate the underlying mechanism involved in hepatic and aortic cholesterol homeostasis.

2. Materials and Methods

2.1. Chemicals. General chemicals were procured from either Sigma-Aldrich Chemical (USA) or Thermo Fisher Scientific (Massachusetts, US). Bradford protein assay kit and total cholesterol assay kit were purchased from GeneCopoeia (Rockville, MD, USA) and Elabscience (Houston, Texas, USA). Rabbit 3-hydroxy-3-methylglutaryl coenzyme A reductase (HMGCR) was supplied by MyBioSource Inc. (San Diego, CA, USA). Standard rabbit pellet was supplied by Gold Coin Feedmills Sdn. Bhd. (Penang, Malaysia), and simvastatin was acquired from Sigma-Aldrich (St. Louis, MO, USA). RNase-free water was purchased from Biohaus Asia Sdn. Bhd. (Selangor, Malaysia). Genome LabGeXP Start

Kit, RNAlaterHiYieldTM RNA Mini Kit, and TRIzol were supplied by Beckman Coulter Inc. (Miami, FL, USA), Real-Biotech Corporation (Taipei, Taiwan), and Invitrogen (California, USA). The MgCl₂ and DNA Taq polymerase were purchased from Thermo Fisher Scientific (Pittsburgh, PA), and the RCL2 solution was obtained from Alphasys (Toulouse, France).

2.2. EBN Sample Preparation. Half-cup-shaped raw-cleaned house edible bird's nest (EBN) was obtained from Blossom View Sdn. Bhd in Terengganu (East Coast of Malaysia). Feathers and other impurities identified during the screening process of the samples were manually removed using tweezers, and the cleaned EBN was kept at 4°C until further usage. The extraction of EBN was conducted by stewing process according to the previous method [13]. The soaked EBN was double-boiled at 100°C for 30 minutes before being cooled to room temperature. The full stew (FS) of EBN was produced from the entire sample of double-boiled EBN without any filtration, while the stew extract (SE) was prepared from double-boiled EBN that had been filtered with a muslin cloth.

2.3. Treatment of Experimentally-Induced Atherosclerosis in Rabbits. Twenty-five healthy male New Zealand white rabbits (8–10 weeks old, 1500–1700 g) were obtained from Goodtree Garden Sdn. Bhd. (Selangor, Malaysia) and housed individually in stainless steel mesh-bottomed cages ($n = 1$) under standard laboratory conditions with a 12-hour dark/light cycle, at 20–24°C and 40–50% relative humidity. The rabbits were randomly assigned to 5 groups ($n = 5$) consisting of two control groups and three treatment groups. The control groups were divided into two groups, namely, normal control (NC): rabbits were maintained on standard rabbit pellet; and high-fat high-cholesterol diet (HFCD): rabbits were fed with a HFC diet containing 69% standard rabbit pellet, 20% palm oil, 10% starch, and 1.0% cholesterol, whereas the treatment groups were divided into three groups, namely, HFCD + FS: rabbits were fed with a similar diet to the HFCD group, with additional supplementation of FS of EBN at 500 mg/kg b.w./day; HFCD + SE: rabbits were fed with a similar diet to the HFCD group, with additional supplementation of SE of EBN at 500 mg/kg b.w./day; and HFCD + STATIN: rabbits were fed a HFC diet and treated with simvastatin at 10 mg/kg b.w./day.

Before starting the study, all rabbits were acclimatized for 1 week on a standard rabbit pellet (ad-libitum) with free access to water. Following acclimatization, the rabbits were fed with a high-fat high-cholesterol (HFC) diet for 12 weeks to induce hypercholesterolemia condition and atherosclerosis. The HFC diet was formulated according to Yida et al. [11] with minor modifications. Accordingly, every kg of HFC diet formulation contained 690 g of rabbit normal pellet (containing 40% carbohydrate, 17% protein, 3% fat, 15% fibre, 2% vitamin/mineral mix, 13% moisture, and 10% ash), 10 g cholesterol, 100 g palm oil, 100 g of margarine, and 100 g starch (to cement the pellet together). The HFC diet pellet was dried in an incubator at 60°C for 48 hr, cut into small equal-

sized cubes, and fed to the rabbits. Doses for EBN supplementation were calculated based on the human equivalent dose (HED) which is about 10 g per day of human consumption as recommended by the EBN supplier. The EBN dose for the experimental animal was determined by the method described by Shin et al. [14]; and 500 mg/kg b.w/day of EBN dosage was set for experimental purposes [14]. The food composition and animal groups are described in Table 1.

EBN and simvastatin were given to the rabbits orally on a daily basis. After 12 weeks of intervention, blood withdrawal (6 ml) through the ear marginal vein under anaesthesia (ketamine/xylazine (35 mg/5 kg b.w-IM)) before sacrificing by pentobarbital (100 mg/kg b.w-IV) was performed on all experimental rabbits. Blood sera were collected after centrifugation of collected blood in serum clot activator tubes with a gel separator. The liver and aorta were carefully excised, weighed, and cleaned. The liver and aorta were preserved in RCL2® solution and stored at -80°C before the RNA extraction protocol whereas the formalin-fixed aorta tissue was kept at room temperature before the histological protocol for examination. All experiments and protocols described in the study were conducted at the experimental animal house of the Faculty of Medicine and Health Sciences, UPM, in accordance with the ethics protocol approved by the Institutional Animal Care and Use Committee of Universiti Putra Malaysia (Animal Ethic approval no. UPM/IACUC/AUP-R009/2017).

2.4. Food Intake and Body Weight. The rabbits received 100 g per day of respective experimental diet, and the food intake of each rabbit was measured by subtracting the amount of leftover food in the food container from the 100 g of the food given. The percentage of body weight gain for each rabbit was calculated as $((\text{final b.w.} - \text{baseline b.w.}) / \text{baseline b.w.}) \times 100$. Food intake and body weight of all rabbits were recorded on a daily and weekly basis, respectively.

2.5. Lipid Profile, Atherogenic Parameters, and Coagulation Function Test. The collected serum and whole blood were sent for analysis of lipid profiles (i.e., TC: total cholesterol, TG: triglycerides, LDL-c: low-density lipoprotein cholesterol, and HDL-c: high-density lipoprotein cholesterol) and the coagulation test (i.e., PT: prothrombin time, APTT: activated partial thromboplastin time, and fibrinogen). Atherogenic indices were calculated as described by Sujatha and Kavitha [15] as follows [15]:

- (i) Castelli risk index I (CRI-I) = $\frac{\text{serum TC}}{\text{serum HDL-c}}$
- (ii) Castelli risk index II (CRI-II) = $\frac{\text{serum LDL-c}}{\text{serum HDL-c}}$
- (iii) Atherogenic index (AI) = $\frac{\text{serum TC} - \text{serum HDL-c}}{\text{HDL-c}}$

2.6. Determination of Tissue Total Cholesterol Content and Hepatic HMGCR. The total cholesterol of the aorta and liver was determined by using a total cholesterol assay kit

following the manufacturer's instruction, and the results were expressed as mg/g wet weight of tissue. Immunoassays were performed by the measurement of hepatic HMGCR by using an ELISA kit according to the manufacturer's instructions, and the result was expressed as mg/g hepatic protein. The hepatic protein content was determined using the Bradford assay kit following the manufacturer's instructions.

2.7. Histopathology of Aorta and Liver Tissues. Histological slides of the aorta and liver tissues were prepared according to the standard histological protocol as described by Andrés-Manzano et al. [16]. The trimmed aorta and liver tissues were placed into specimen cassettes prior to fixation, dehydration and clearing, paraffin infiltration, and tissue embedding. Then, the tissue sectioning at a thickness of $5\ \mu\text{m}$ thickness was conducted using a microtome (Leica Biosystem, Nussloch, Germany), followed by staining with Hematoxylin and Eosin (H&E) stain. To evaluate the histopathological changes, the slides were examined under a MOTIC BA410 light microscope (Motic Hong Kong Ltd., Kowloon, Hong Kong). Atherosclerotic plaque formation was evaluated by measuring the thickness of tunica intima and tunica media, and the ratio of tunica intima to tunica media was calculated.

2.8. Hepatic and Aortic Gene Expression Analyses. The total RNA of liver and aorta tissues was extracted using a total RNA isolation kit (RBC Biotech), with minor modifications to the manufacturer's instructions. In brief, 50 mg of frozen tissue were homogenized in lysis buffer (liver) or TRIzol (aorta) to lyse the cells and the RNA concentration was determined by using a NanoDrop spectrophotometer (Thermo Scientific Nanodrop, NanoDrop Technologies, Wilmington, DE, USA). Genome Lab eXpress Profiler software was employed to design the primer based on the *Oryctolagus cuniculus* sequence adopted from the National Center for Biotechnology Information Gen Bank Database (<https://www.ncbi.nlm.nih.gov/nucleotide/>). The primer sequences for 8 genes of interest related to cholesterol homeostasis for the rabbit hepatic and aortic multiplex panel are shown in Table 2. Primers were supplied by Integrated DNA Technologies (Singapore) and diluted with RNase-free water to concentrations of 500 nM (reverse primer) and 200 nM (forward primers).

The RNA samples ($50\ \text{ng}/\mu\text{l}$) were subjected to reverse transcription (RT) and multiplex polymerase chain reaction (PCR) using XP Thermal Cycler (BIOER Technology, Germany) according to GenomeLab™ GeXP Start Kit (Beckman Coulter, Inc. Miami, FL, USA). The cDNA was synthesized at the following conditions: 48°C for 1 min, 42°C for 60 min, 95°C for 5 min, and 4°C hold. For amplification, the condition was set as follows: 95°C for 10 min, followed by 34 cycles of 94°C for 30 sec, 55°C for 30 sec, 70°C for 1 min, and 4°C hold. The PCR amplification products ($1\ \mu\text{l}$) were mixed with $38.5\ \mu\text{l}$ of

TABLE 1: Food composition and animal groups.

Animal groups	Standard pellet (%)	Cholesterol (%)	Palm oil + margarine (%)	Starch (%)	Others (daily dose)
NC	100				Distilled water
HFCD	69	1	20	10	Distilled water
HFCD + STATIN	69	1	20	10	Simvastatin ^a
HFCD + FS	69	1	20	10	FS of EBN ^b
HFCD + SE	69	1	20	10	SE of EBN ^b

NC, normal control; HFCD, high-fat high-cholesterol diet; EBN, edible bird's nest; FS, full stew; SE, stew extract; mg/kg b.w./day, milligram per kilogram of body weight per day. ^aDose at 10 mg/kg b.w. ^bDose at 500 mg/kg b.w.

TABLE 2: Gene name, accession number, and primer sequences used in the GeXP multiplex analysis of rabbit hepatic and aortic genes.

Gene name (accession no.)	Primer sequence (with universal tag)
LOX-1 (NM_001082633.1)	F: AGGTGACACTATAGAATACCCCACTTGTTCAGATT R: GTACGACTCACTATAGGGACTTCAAATCACTCTGATCTC
CD36 (XM_002712016.3)	F: AGGTGACACTATAGAATACATTTGATTGAAAAATCCTT R: GTACGACTCACTATAGGGATCTGGTTCCTTATTCACGATT
LDLR (NM_001278865.1)	F: AGGTGACACTATAGAATACTGCGAAGATATCAATGAGT R: GTACGACTCACTATAGGGATACTCGCTACGGTCCA
ABCA1 (XM_008257418.2)	F: AGGTGACACTATAGAATAAGGCAGAGGAGGAGAG R: GTACGACTCACTATAGGGACAAGGTGCCATCTGA
LCAT (NM_001082190.1)	F: AGGTGACACTATAGAATACGATAATACCAGGGTTG R: GTACGACTCACTATAGGGACAGCTTGTGTGTCTAGG
CYP7A1 (NM_001170929.1)	F: AGGTGACACTATAGAATAATCAAACACAACCTGAATGAC R: GTACGACTCACTATAGGGATAACTGCGGATAAAGAGCTA
LXR α (NM_001184956.1)	F: AGGTGACACTATAGAATATGTTTCTCCTGACTCTGC R: GTACGACTCACTATAGGGACTTCTCCGCTTTTGTG
PPAR γ (NM_001082148.1)	F: AGGTGACACTATAGAATACGAACTCTTGATTTTGAAGT R: GTACGACTCACTATAGGGATGACTTCTTTTATGGATGACT
ACTB ^a (NM_001101683.1)	F: AGGTGACACTATAGAATAAGGCGGACTGTTAGAGC R: GTACGACTCACTATAGGGACTCAGGATATTTGGAATGACT
GAPDH ^{a*} (NM_001082253.1)	F: AGGTGACACTATAGAATACTCATTTCTGGTATGACAA R: GTACGACTCACTATAGGGATCGAGACTTTATTGATGGTT
KanR ^b	F: AGGTGACACTATAGAATAATCATCAGCATTGCATTTCGATTCCTGTTTG R: GTACGACTCACTATAGGGAATCCGACTCGTCCAACATC

^aHousekeeping gene. ^bInternal control. ^{*}Normalization gene; F, forward primer sequence; R, reverse primer sequence. LOX-1, lectin-like oxidized low-density lipoprotein receptor-1; CD36, cluster of differentiation 36; LDLR, low-density lipoprotein receptor; ABCA1, ATP-binding cassette subfamily A member 1; LCAT, lecithin-cholesterol acyltransferase; CYP7A1, cytochrome P450 family 7 subfamily A member 1; LXR α , liver X receptor alpha; PPAR γ , peroxisome proliferator-activated receptor gamma; GAPDH, glyceraldehyde 3-phosphate dehydrogenase; ACTB, beta (β -actin); KanR, kanamycin resistant.

sample loading solution and 0.5 μ l of DNA size standard (Beckman Coulter, Inc. Miami, FL, USA) in a sample loading plate, before being separated by the GeXP genome lab genetic analysis system. The optimization step was performed to standardize the peak of detection for each gene. Subsequently, the fragment analysis module and the eXpress Profiler program were used to analyze the results. The results are expressed as the ratio of the mRNA of interest to the GAPDH mRNA.

2.9. Statistical Analysis. Statistical analysis was performed using SPSS version 28.0. All results were expressed as the mean \pm standard error of the mean (SEM). The data were statistically treated by analysis of variance (ANOVA) and Tukey's test with $p < 0.05$ considered as statistically significant.

3. Results and Discussion

3.1. Characterization and Bioactive Compound of EBN. In our previous studies, we found that EBN is high in nutritional value and bioactive components [13, 17]. The nutritional composition analysis of the EBN had revealed that it comprises of high protein (>50%) and carbohydrates (>20%). In addition, the major bioactive compound detected in EBN is glycoprotein sialic acid with 7.91% (FS) and 8.47% (SE). Further exploration of its monomeric amino acid contents has identified that the major amino acids in EBN were glutamic acid, aspartic acid, serine, and valine. Protein profiling has confirmed that EBN from this study contains seven parent proteins, namely, 78 kDa glucose-regulated protein, lysyl oxidase-3, mucin-5AC-like, acidic mammalian chitinase-like (AMCase-like), 45 kDa calcium-binding protein, nucleobindin-2, and ovoidinhibitor. The findings of

nutritional composition, protein profile, and sialic acid content show that EBN is a good source of protein and glycoprotein, potentially exhibiting nutritional and medicinal properties. Based on the protein and carbohydrate composition, FS and SE of half-cup EBN were selected and used in this study.

3.2. Caloric Intake and Body Weight Gain following EBN Supplementation. The effects of FS and SE of EBN on weight changes and caloric intake of HFC diet-fed rabbits are shown in Table 3. There was no significant intragroup change in basal body weights prior to the intervention ($p > 0.05$). The HFCD group gained significantly more weight ($35.85 \pm 0.22\%$) as compared to other experimental groups after 12 weeks of intervention on the respective diet ($p < 0.05$). In addition, there was no difference in weight gain between the NC, HFCD + FS, and HFCD + SE groups with the increment in body weight ranging from 23.89 to 25.29% ($p > 0.05$). Compared to the NC group, the increment of body weight in the HFCD group could be explained by the difference in diet composition between HFCD (carbohydrate: 38%; fat: 23%) and standard rabbit pellet (carbohydrate: 42%; fat: 3%). According to Alarcon et al. [18], the administration of a diet containing more than 18% of fat for 6 weeks resulted in an increase in body weight and visceral abdominal fat in rabbits. Therefore, the increase in body weight could have been due to increased lipid accumulation in the body tissue of the rabbits in the HFCD group. However, significantly the lowest body weight gain was shown by the HFCD + STATIN group with $20.14 \pm 0.19\%$, which could be contributed by the weight-loss properties of simvastatin [19].

As shown in Table 3, rabbits in the NC group showed a high caloric intake in their diet as compared to other groups ($p < 0.05$). This is most likely due to the food being poorly accepted or other factors related to the level of activity or stress in rabbits receiving the HFC diet regime. Despite the similar caloric intake between treatment groups (except for the HFCD + STATIN group), rabbits supplemented with EBN showed significantly less weight gain than rabbits administered with the HFC diet alone ($p < 0.05$). The presence of glycoprotein sialic acid, protein nucleobindin-2, and fibre components in FS and SE of EBN could probably deliver the potential of EBN in weight management [13, 17]. The effects of these EBN components on body weight changes have been reported in the literature involving *in vivo* models [20–22]. Apart from the nutrition components mentioned above, Hou et al. [23] have claimed that protein lactoferrin and ovotransferrin in EBN significantly reduced the food intake and body weight increment in ovariectomized-induced menopause in rats, as low level of estrogen in these rats could promote weight gain. These findings support the weight-modulating properties of EBN in HFC diet-fed rabbits in this study.

3.3. Improved Lipid Profiles and Atherogenic Indices with EBN Supplementation. Table 4 shows the changes in serum TC, LDL-c, HDL-c, and TG values in rabbits supplemented with

simvastatin and EBN. At the end of the intervention, the serum TC (22.90 ± 0.07 mmol/L) and LDL-c levels (16.43 ± 1.35 mmol/L) were markedly elevated in the HFCD group as compared to the NC group ($p < 0.05$). The results suggested that hypercholesterolemia induced in the rabbit model had been successfully established. In comparison to the HFCD group, cosupplementation of EBN with the HFC diet effectively lowered both serum TC and LDL-c of hypercholesterolemic rabbits ($p < 0.05$). The anti-hypercholesterolemic of FS and SE was comparable to the simvastatin treatment (HFCD + STATIN group) in reducing the serum TC level ($p > 0.05$).

Meanwhile, both the HFCD + SE and HFCD + STATIN groups reduced serum LDL-c levels in hypercholesterolemic rabbits in a similar manner (20.57% vs. 24.77%; $p > 0.05$). In addition, the serum HDL-c level in the HFCD + FS group was markedly increased as compared to that in the HFCD group ($p < 0.05$), and this enhancing property was comparable to simvastatin treatment (HFCD + STATIN group, $p > 0.05$). However, there was no significant difference in the serum HDL-c level observed between HFCD + SE and HFCD groups ($p > 0.05$), indicating that a combination of the water-soluble and insoluble fractions in FS of EBN is essential for HDL-c improvement.

The level of serum TG in the HFCD + STATIN group was comparable to the NC group ($p > 0.05$), indicating that simvastatin treatment was able to maintain circulating TG at a normal level. This could be related to low-calorie intake (low percentage of fat) by the rabbits in the HFCD + STATIN group aforementioned. Interestingly, both HFCD + FS and HFCD + SE groups showed a marked reduction in serum TG levels as compared to other experimental groups ($p < 0.05$). The increase in serum TG level in the HFCD group indicated that the HFC diet leads to the accumulation of fat in the blood, and EBN supplementation is able to minimize the circulating TG level. EBN groups tackled different lipid parameters, whereby SE and FS worked superior on reducing serum TC and HDL-c, respectively, than those achieved by the simvastatin drug. However, despite the fact that HDL-c increased with a slight statistical significance, the increasing fold of LDL-c was more prominent. It is hypothesized that there would be some compensatory increase in HDL-c to remove extra cholesterol, but the increase is significantly less than that of LDL-c.

The Castelli risk index I (CRI) has been demonstrated to accurately reflect the formation of coronary plaques and the thickness of the intima-media in the carotid arteries of young adults [24]. Meanwhile, the CRI-II or LDL-c/HDL-c ratio has been related to predicting the coronary artery disease (CAD) risk [25]. The atherogenic index (AI) is a measurement of cholesterol in the LDL-c, VLDL-c, and IDL-c lipoprotein fractions in comparison to good cholesterol or HDL-c, whereby it may reflect the atherogenic potential of the whole lipoprotein fraction. In this study, the HFC diet feeding increased the CRI-I, CRI-II, and AI values of the HFCD group by 38%, 211%, and 38%, respectively ($p < 0.05$), when compared to the NC group. In comparison to the HFCD group, EBN supplementation for 12 weeks produced a low risk of CHD by reducing the CRI-I (FS: 22.8%; SE: 21.3%),

TABLE 3: Bodyweight gain and caloric intake of experimental rabbits after 12 weeks of intervention.

Groups	Baseline body weight (kg)	Final body weight (kg)	Body weight gain (%)	Caloric intake (kcal/b.w/day)
NC	1.905 ^a ± 0.02	2.363 ^b ± 0.07	25.29 ^b ± 0.17	314.89 ^a ± 0.68
HFCD	1.943 ^a ± 0.09	2.620 ^a ± 0.09	35.85 ^a ± 0.22	271.28 ^b ± 3.41
HFCD + STATIN	1.911 ^a ± 0.18	2.316 ^b ± 0.31	20.14 ^c ± 0.19	250.78 ^c ± 3.37
HFCD + FS	1.940 ^a ± 0.13	2.371 ^b ± 0.12	23.89 ^b ± 0.18	269.94 ^b ± 2.64
HFCD + SE	1.863 ^a ± 0.04	2.323 ^b ± 0.07	24.36 ^b ± 0.16	275.61 ^b ± 4.06

Values shown are expressed as the mean ± standard error of the mean (SEM, $n = 5$). Different letters within the same column indicate significant differences ($p < 0.05$, $a > b > c$). NC, normal control; HFCD, high-fat high-cholesterol diet; STATIN, simvastatin; FS, full stew of EBN; SE, stew extract of EBN.

TABLE 4: Serum lipid profiles and atherogenic indices over the 12 weeks of edible bird's nest intervention on high-fat high-cholesterol fed rabbits.

Groups	Lipid profiles				Atherogenic indices		
	TC (mmol/L)	LDL-c (mmol/L)	HDL-c (mmol/L)	TG (mmol/L)	CRI-I	CRI-II	AI
NC	0.97 ^d ± 0.15	0.29 ^d ± 0.13	0.23 ^c ± 0.06	1.90 ^b ± 0.36	3.78 ^c ± 0.50	1.23 ^c ± 0.31	3.05 ^c ± 0.49
HFCD	22.90 ^a ± 0.07	16.43 ^a ± 1.35	4.38 ^b ± 0.04	2.31 ^a ± 0.37	5.22 ^a ± 0.03	3.83 ^a ± 0.16	4.22 ^a ± 0.03
HFCD + STATIN	21.06 ^{b,c} ± 0.10	12.36 ^c ± 0.42	5.92 ^a ± 0.26	2.08 ^b ± 0.61	4.05 ^b ± 0.49	2.50 ^b ± 0.35	3.57 ^b ± 1.48
HFCD + FS	21.34 ^b ± 0.49	14.94 ^b ± 0.16	6.11 ^a ± 0.12	1.29 ^c ± 0.14	4.03 ^b ± 0.12	2.47 ^b ± 0.13	2.81 ^c ± 0.37
HFCD + SE	20.27 ^c ± 0.07	13.05 ^{b,c} ± 1.01	4.41 ^b ± 0.44	1.33 ^c ± 0.59	4.11 ^b ± 0.43	2.84 ^b ± 0.17	3.40 ^b ± 0.40

Values shown are expressed as the mean ± standard error of the mean (SEM, $n = 5$). Different letters mean significant differences between groups ($p < 0.05$, $a > b > c > d$). NC, normal control; HFCD, high-fat high-cholesterol diet; STATIN, simvastatin; FS, full stew of EBN; SE, stew extract of EBN; TC, total cholesterol; LDL-c, low-density lipoprotein cholesterol; HDL-c, high-density lipoprotein cholesterol; TG, triglyceride; CRI-I, Castelli risk index I; CRI-II, Castelli risk index II; AI, atherogenic index.

CRI-II (FS: 35.5%; SE: 25.8%), and AI (FS: 33.4%; SE: 19.4%) values in respective experimental groups. These data suggested that EBN potentially reduces the risk of cardiovascular disease and atherosclerosis by improvement in lipid profiles, with an alteration in LDL-c and HDL-c possibly contributing to this process. A similar finding was also reported that EBN was found to improve lipid profile by lowering serum TC and LDL-c, while increasing HDL-c levels in high-fat diet-fed rats, even better than simvastatin [11].

3.4. EBN Reduced Hepatosteatosis and Stabilized the Atherosclerotic Plaque Formation. Histological sections on the liver tissue of experimental animals are shown in Figure 1. Rabbits in the NC group displayed a normal structure of liver tissue with the hepatic cords surrounding central veins with regularly oriented sinusoids (Figure 1(a)). The hepatic parenchyma was shown to exhibit focal macrovesicular steatosis, which is generally observed in the normal liver since the liver serves as a key gland for nutritional storage and metabolism [26]. The changes in the liver structure after 12 weeks of dietary intervention can be noticed microscopically, as shown in Figures 1(b)–1(e). The administration of the HFC diet resulted in a remarkable change in liver histology of the HFCD group with the presence of multiple macrovesicular steatosis in hepatocytes, as well as significant ballooning of the liver cells (Figure 1(b)). These histopathological findings are consistent with the observation by Ashry et al. [27], who captured the same hepatic architecture with the presence of large lipid vacuoles in hypercholesterolemic rabbits. The significant appearance of macrovesicular steatosis in the HFCD group indicated that a cholesterol-enriched diet potentially caused fatty liver.

The liver image from the HFCD + STATIN group was found to restore the normal histological appearance of the liver cords, central vein, portal areas, and sinusoids, as well as a significant reduction in steatosis (Figure 1(c)). A similar feature of the liver histology was exhibited by the HFCD + FS (Figure 1(d)) and HFCD + SE (Figure 1(e)) groups. The hepatic steatosis could be due to lipid accumulation in the hepatocytes, and there are direct correlations between serum TG and NAFLD [28]. The sialic acid content and protein nucleobindin-2 identified in the EBN from this study may contribute to the reduction of fat accumulation in the hepatocytes [13]. The administration of exogenous sialic acid has been shown to reduce 26.7% lipid deposition in the liver of atherosclerotic mice fed with a HFC diet [29]. Meanwhile, nucleobindin-2 reduces hepatic lipid accumulation in diet-induced obese mice by directly acting on hepatocytes, and this effect is independent of food intake [30]. Thus, it can be suggested that the administration of EBN protects the liver against hypercholesterolemia-induced hepatosteatosis.

The images of H&E-stained rabbits' aorta are depicted in Figure 2, and the image of the NC group exhibited the presence of an intact and normal aortic tunica intima with orderly oriented endothelial cells (Figure 2(a)). Histological examination of the aortic tissue of the hypercholesterolemic rabbit groups revealed an apparent thickening of the tunica intima, which was filled with foam cells, and resulted in a significant reduction of the aortic vascular lumens (Figures 2(b)–2(f)). The smooth muscle cells within tunica media were replaced by a granular white substance precisely known as a fatty streak in the hypercholesterolemic rabbits with different severity as follows: HFCD > HFCD + SE > HFCD + FS > HFCD + STATIN.

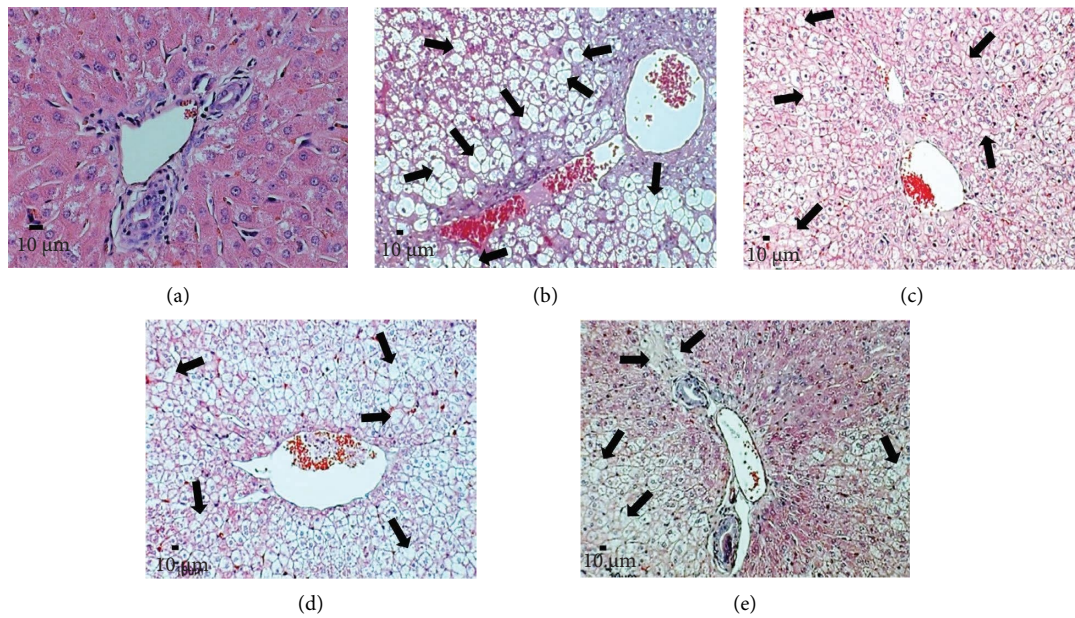


FIGURE 1: Effects of EBN on hepatic histopathological changes of HFC diet-induced hypercholesterolemia in rabbits. The images (a–e) were examined under a light microscope at 400x (a) and 200x (b–e) magnifications. Black arrows indicate lipid droplets in liver cells. Scale bar = 10 μ m. NC: normal control; HFCD: high-fat high cholesterol diet; STATIN: simvastatin; FS: full stew of EBN; SE: stew extract of EBN. (a) NC, (b) HFCD, (c) HFCD + FS, (d) HFCD + SE, and (e) HFCD + STATIN.

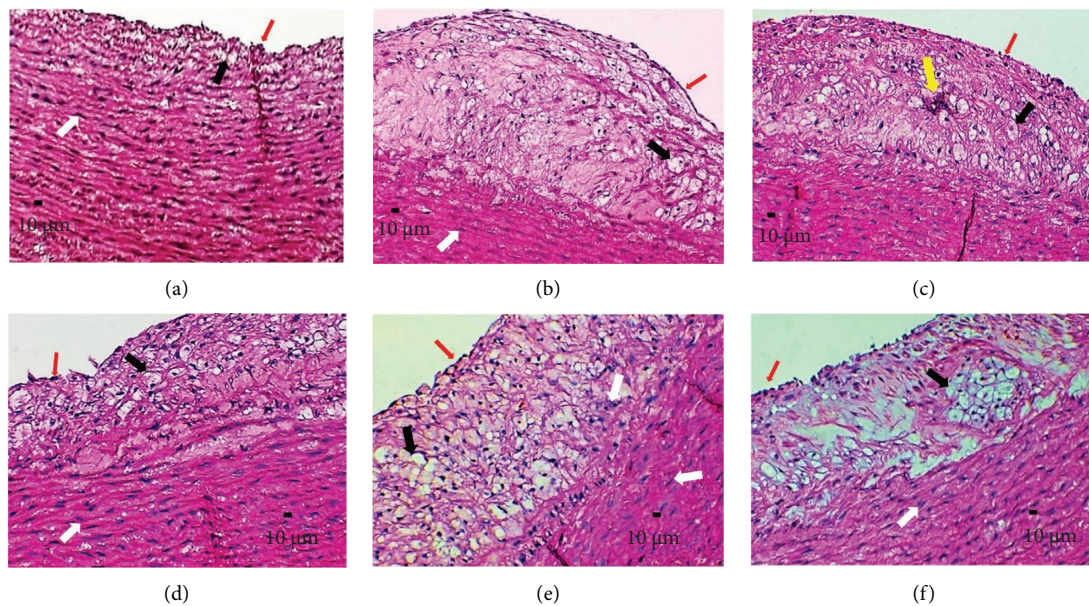


FIGURE 2: Histopathological overview of the fatty streak area in the HFC diet-induced atherosclerosis in rabbits (a–f) examined under a light microscope at 200x magnification. Red arrows indicate endothelial cells, black arrows indicate foamy cells, yellow arrow indicates calcium deposition, and white arrows indicate smooth muscle cells. Scale bar = 10 μ m. NC: normal control; HFCD: high-fat high-cholesterol diet; STATIN: simvastatin; FS: full stew of EBN; SE: stew extract of EBN. (a) NC, (b) HFCD, (c) HFCD, (d) HFCD + FS, (e) HFCD + SE, and (f) HFCD + STATIN.

As expected, a substantial lipid core (Figure 2(b)) and calcification (Figure 2(c)) in the intimal layer of the aorta would be highly expressed in the HFCD group. In comparison to the NC group, the HFCD + FS (Figure 2(d)) and HFCD + STATIN (Figure 2(f)) groups resulted in mild

atheromatic lesions with a thin layer of plaque in the aorta. Meanwhile, the HFCD + SE group resulted in more profound plaques (Figure 2(e)). Microscopic examinations of the aorta wall indicated the superiority of FS in reducing plaque formation as compared to SE of EBN while

cotreatment with SE on HFCd-induced atherosclerosis rabbits had a less significant effect on decreasing the size of atherosclerotic plaques developed in the aortic wall but might assist with plaques stabilization.

The measurement for tunica intima and tunica media thickness was performed for each rabbit with three aortic cross-sections as depicted in Figures 3(a)–3(e). As illustrated in Figure 3(f), the intima thickness of the aorta was significantly increased in the HFCd group, when compared to the NC group ($452.63 \pm 15.88 \mu\text{m}$ vs. $25.30 \pm 4.14 \mu\text{m}$; $p < 0.05$). EBN supplementation on rabbits fed with a HFC diet resulted in a significant reduction ($p < 0.05$) of tunica intima thickness by 63% (HFCd + FS group: $169.60 \pm 22.92 \mu\text{m}$) and 47% (HFCd + SE group: $240.57 \pm 28.96 \mu\text{m}$), respectively. The tunica intima thickness of the aorta for the HFCd + FS group was comparable to the HFCd + STATIN group ($183.95 \pm 6.13 \mu\text{m}$) ($p < 0.05$). There was no significant difference observed between the experimental groups (except the HFCd group) with regard to media thickness (Figure 3(g)) ($p < 0.05$).

In comparison to the NC group, it can be observed that the I/M ratio of the aorta of experimental rabbits in the HFCd group significantly increased (0.07 ± 0.03 vs. 1.10 ± 0.16 ; $p < 0.05$) after 12 weeks of HFC diet feeding. Meanwhile, EBN supplementation markedly reduced the I/M ratio of the aorta section (FS: 0.62 ± 0.09 ; SE: 0.80 ± 0.23) in the hypercholesterolemic rabbits ($p < 0.05$). The I/M ratio of the aorta in the HFCd + FS group was comparable with the HFCd + STATIN group (0.70 ± 0.36 ; $p > 0.05$). In agreement with the literature [31, 32], histopathological examination in the present study conveyed that the HFC diet is responsible for the thickening of the tunica intima layer. Hypercholesterolemic rabbits supplemented with EBN and simvastatin confirmed the thinner aortic tunica and managed to stabilize plaque progression as compared to the HFCd group. This result suggests that 1.0% cholesterol incorporated into a high-fat diet promoted atherogenesis and EBN supplementation delayed the progression of atherosclerosis.

3.5. EBN Improved the Coagulation Status of Hypercholesterolemic Rabbits. Figure 4 reveals the effect of EBN on the coagulation status of experimental rabbits. The PT (Figure 4(a)) and APTT (Figure 4(b)) were significantly shorter in the HFCd group with recorded times of 6.85 ± 0.50 sec and 20.30 ± 1.71 sec, respectively. In comparison to the HFCd group, there was a substantial increase in both PT and APTT as recorded for the HFCd + FS (PT: 8.90 ± 0.37 sec; APTT: 24.10 ± 3.22 sec) and HFCd + SE (PT: 9.20 ± 0.77 sec; APTT: 23.63 ± 0.68 sec) groups, which were comparable with the HFCd + STATIN group ($p > 0.05$). The Fb level (Figure 4(c)) was markedly increased following the HFC diet feeding (5.00 ± 1.33 sec; $p < 0.05$) and was found to be reduced ($p < 0.05$) by EBN supplementation and simvastatin treatment on hypercholesterolemic rabbits (HFCd + FS: 2.00 ± 0.33 g/L; HFCd + SE: 3.00 ± 0.81 g/L; HFCd + STATIN: 3.00 ± 0.67 g/L), with no difference observed between HFCd + SE and HFCd + STATIN groups ($p > 0.05$). No difference ($p > 0.05$) was observed in the Fb level between HFCd + FS and NC groups (2.00 ± 0.00 g/L).

Significant increases in clotting factors such as prothrombin, VII, and X were observed in high cholesterol-fed rabbits [33], and PT and APTT prolongation may also be caused by the suppression of these intrinsic coagulation factors. Findings from this study were in accordance with the previous literature that reported prolonged PT and APTT in HFCd-induced coagulation in rats supplemented with EBN and its bioactive sialic acid [12, 34]. Moreover, sialic acid is found on the surface of vascular endothelium and erythrocytes, thereby increasing the negative charge that prevents blood clotting [35].

The coagulation proteins are commonly present in early atherosclerotic lesions compared to advanced atherosclerotic lesions [36], thus suggesting that these coagulation proteins play a significant role in the initial development of atherosclerosis, rather than being involved exclusively in thrombus formation in unstable plaques. Furthermore, the elevated Fb serum concentration is considered one of the proatherogenic indicators that may accelerate the progression of atherosclerotic plaque formation through several mechanisms of action such as increasing the severity of inflammation, platelet activation, facilitating LDL-c absorption on the vessel wall, and enhancing infiltration of macrophage into the arterial intima [37, 38]. Therefore, improving coagulation status is one of the possible approaches to prevent atherosclerosis. It can be suggested that the HFC diet may promote hypercoagulation partially due to the induction of hypercholesterolemia and that EBN may have mitigated hypercoagulation partly by regulating cholesterol levels.

3.6. Effect of EBN on Cholesterol Accumulation and Gene Expression in Liver and Aorta Tissues. In order to identify the mechanism underlying hypercholesterolemia and atherosclerotic plaque formation, the cholesterol accumulation and transcriptional analysis related to cholesterol metabolism were determined in the liver and aorta of rabbits. The level of hepatic HMGCR (Figure 5(a)) and hepatic total cholesterol (TC) (Figure 5(b)) in the hypercholesterolemic rabbits was increased by 3.3-fold and 7.6-fold, respectively, as compared to the NC group ($p < 0.05$). Meanwhile, cosupplementation with EBNs was found to reduce the hepatic HMGCR (HFCd + FS: 1.3-fold; HFCd + SE: 1.4-fold) and hepatic TC (HFCd + FS: 1.6-fold; HFCd + SE: 1.7-fold) levels of the hypercholesterolemic rabbits and were comparable to simvastatin treatment ($p > 0.05$). A reduced HMGCR activity decreases TC production in the liver and lowers serum cholesterol levels [39]. This is in line with the reduction in serum TC levels in experimental groups following the dietary interventions of EBN and simvastatin in this study.

A similar effect on cholesterol accumulation was observed in the aortic tissue of hypercholesterolemic rabbits (Figure 5(c)), where EBN reduced the aortic TC level by 59% and 44% in HFCd + FS and HFCd + SE groups, respectively ($p < 0.05$). However, rabbits supplemented with FS of EBN showed the lowest aortic TC among hypercholesterolemic rabbits which were significantly different from SE and simvastatin treatment ($p < 0.05$), and the efficacy of FS in

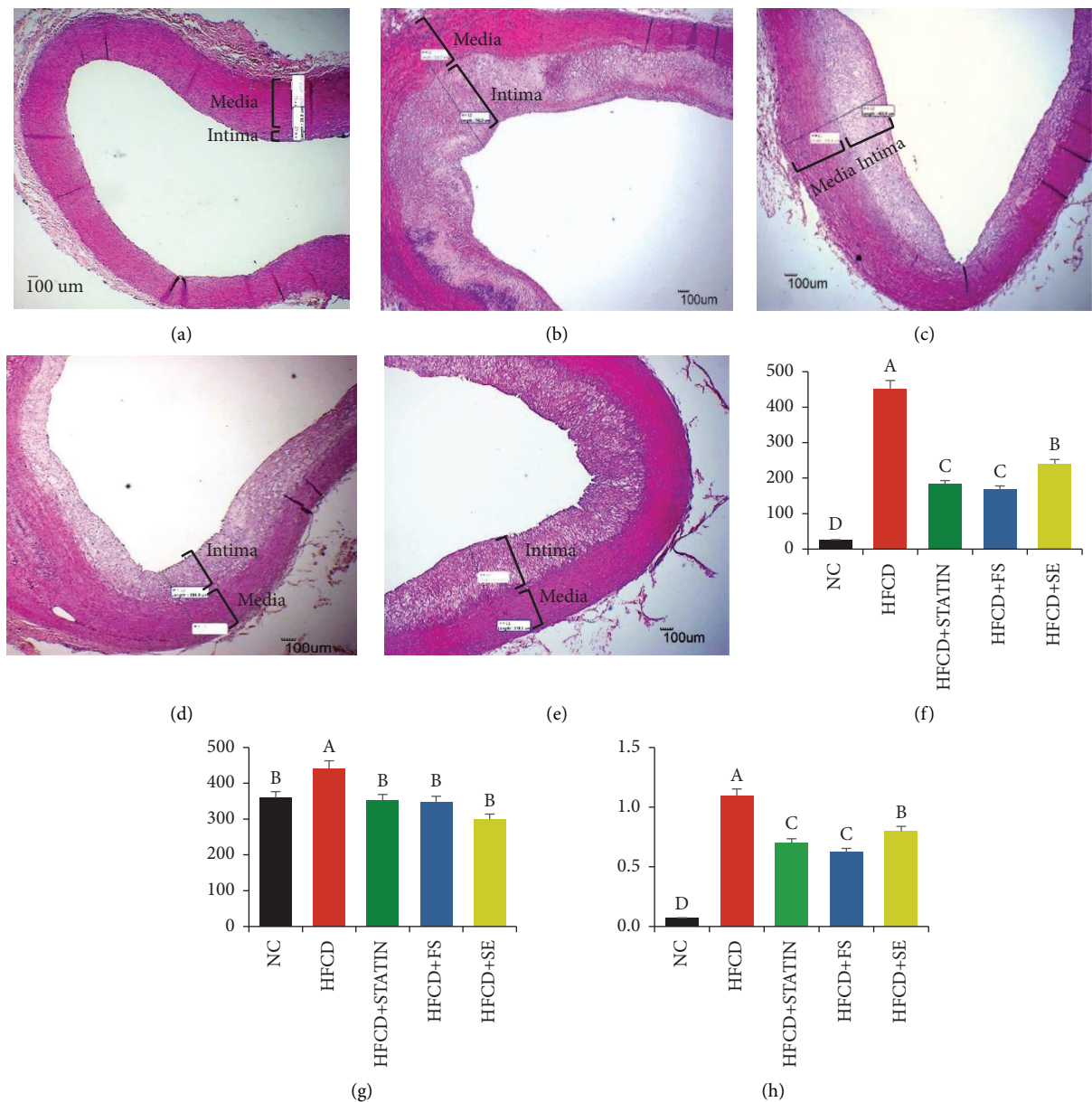


FIGURE 3: Effects of EBN on plaque formation in the hypercholesterolemic rabbits. Hematoxylin and Eosin (H&E) staining was performed on aorta tissue sectioning and images (a–e) were examined under the light microscope at 40x magnification. Atheroma plaque formation was measured based on (f) tunica intima thickness, (g) tunica media thickness, and (h) intima to media ratio. Values shown are expressed as the mean \pm standard error of the mean (SEM, $n = 5$). Different letters mean significant differences between groups ($p < 0.05$, $a > b > c > d$). Scale bar = 100 μm . NC: normal control; HFCD: high-fat high-cholesterol diet; STATIN: simvastatin; FS: full stew of EBN; SE: stew extract of EBN. (a) NC, (b) HFCD, (c) HFCD + STAT, (d) HFCD + FS, (e) HFCD + SE, (f) intima thickness (μm), (g) media thickness (μm), and (h) intima/media ratio.

lowering the aortic TC was coherent with the reduction of tunica intima/media thickness of the aorta in the HFCD + FS group (Figure 3(d)). In accordance with the previous findings [40, 41], administration of the HFC diet significantly increased hepatic TC content, which was strongly correlated with the aortic TC level ($r = 0.963$; $p < 0.05$) of the hypercholesterolemic rabbits in this study. Thus, EBN supplementation could exert a similar effect to that of simvastatin, by lowering hepatic TC via inhibiting the HMGCR activity and subsequently reducing cholesterol accumulation in the aorta.

As illustrated in Figure 6(a), HFC diet feeding altered the transcription of cholesterol-mediated receptors in the liver. In comparison to the NC group, HFC diet administration has suppressed hepatic LDLR expression by 1.7-fold. Meanwhile, EBN supplementation (both FS and SE) has increased the hepatic LDLR expression of hypercholesterolemic rabbits by 2.0-fold ($p < 0.05$), as compared to the HFCD group. As a standard drug used for hypercholesterolemia, simvastatin treatment showed a substantially higher hepatic LDLR expression than other

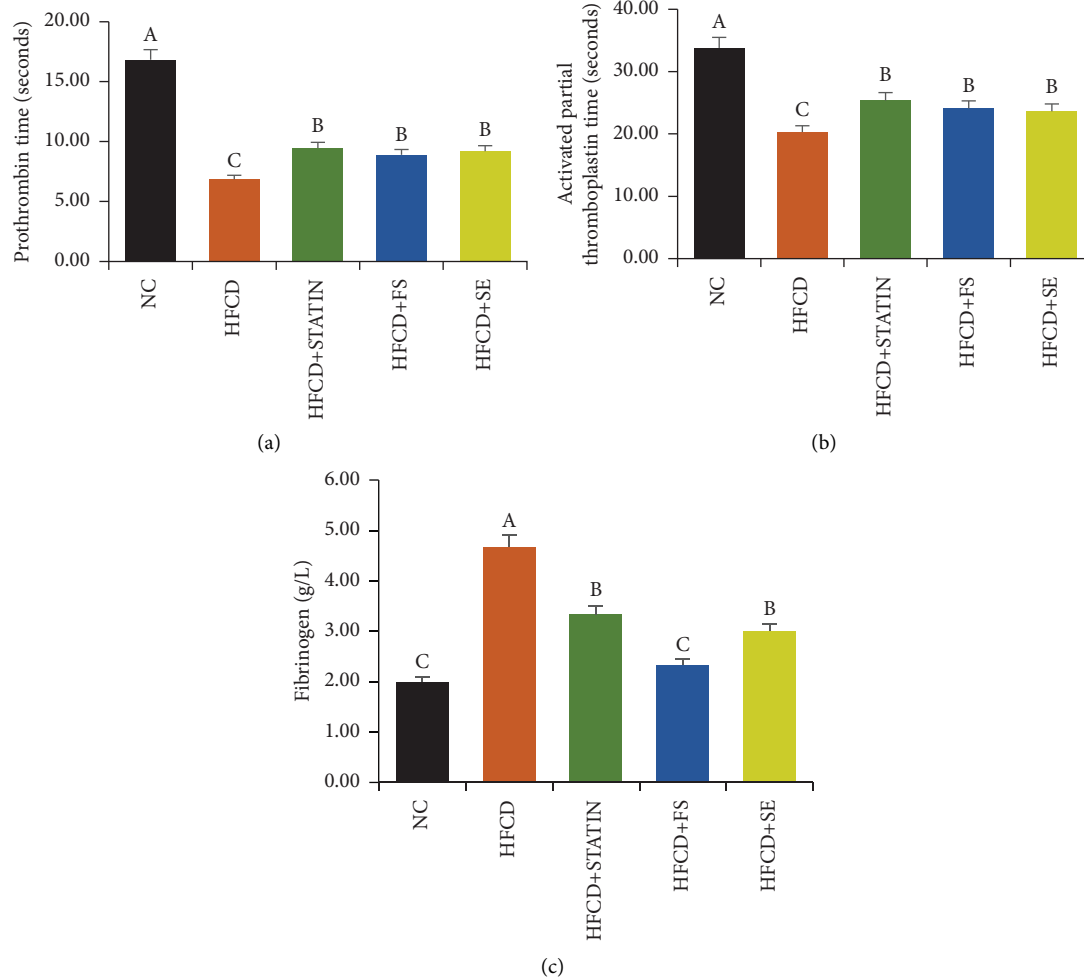


FIGURE 4: Effects of EBN on (a) prothrombin time, (b) activated partial thromboplastin time, and (c) fibrinogen levels in the hypercholesterolemic rabbits. Values shown are expressed as the mean \pm standard error of the mean (SEM, $n = 5$). Different letters mean significant differences between groups ($p < 0.05$, $a > b > c$). NC: normal control; HFCD: high-fat high-cholesterol diet; STATIN: simvastatin; FS: full stew of EBN; SE: stew extract of EBN.

hypercholesterolemic groups ($p < 0.05$). In contrast, there was no significant difference in the transcription of aortic LDLR (Figure 7(a)) between all experimental groups ($p > 0.05$). This implied that LDL-c transendothelial transport in the aorta is mediated by receptors other than LDLR [42].

As shown in Figure 6(a), the uptake of oxLDL in the liver was predominantly mediated by the LOX-1 scavenger receptor, in order of, HFCD + STATIN > HFCD + SE > HFCD + FS > HFCD > NC groups ($p < 0.05$), with insignificantly different hepatic CD36 expression levels between all experimental groups ($p > 0.05$). On the other hand, Figure 7(a) show an upregulation of both LOX-1 (2.8-fold) and CD36 (8.3-fold) expression in the aorta of the HFCD group as compared to the NC group ($p < 0.05$). The alteration of these scavenger receptors by the HFC diet in the liver and aorta was reversed by cosupplementation with EBN and simvastatin treatment. EBN supplementations enhanced the hepatic LOX-1 expression (HFCD + SE: 2.1-fold; HFCD + FS: 2.1-fold; $p < 0.05$) and downregulated the aortic LOX-1 (HFCD + FS: 1.7-fold; HFCD + SE: 1.5-fold; $p < 0.05$)

and aortic CD36 (HFCD + FS: 2.2-fold; HFCD + SE: 1.9-fold; $p < 0.05$) expressions.

In contrast, the CD36 mRNA expression was greatly expressed than the LOX-1 mRNA expression in the aorta of hypercholesterolemic rabbits. According to Schaeffer et al. [43], LOX-1 knockout in macrophages did not result in substantial differences in oxLDL uptake compared to wild-type cells. Thus, under normal settings, LOX-1 has a negligible effect on the intake and degradation of oxLDL by macrophages, most likely due to the large involvement of the CD36 receptor. Therefore, in this study, the major receptors involved in oxLDL uptake in the liver and aorta of hypercholesterolemic rabbits were LOX-1 and CD36, respectively. The enhancement of hepatic LOX-1 by EBN remarkably increased the oxLDL clearance by the liver, subsequently reducing the oxLDL uptake by aortic CD36 receptor in hypercholesterolemic rabbits.

As depicted in Figures 6(b) and 7(b), rabbits administered with a HFC diet showed no changes in both hepatic and aortic ABCA1 expression in the HFCD group, when compared with the NC group ($p < 0.05$). However, upregulation of LCAT

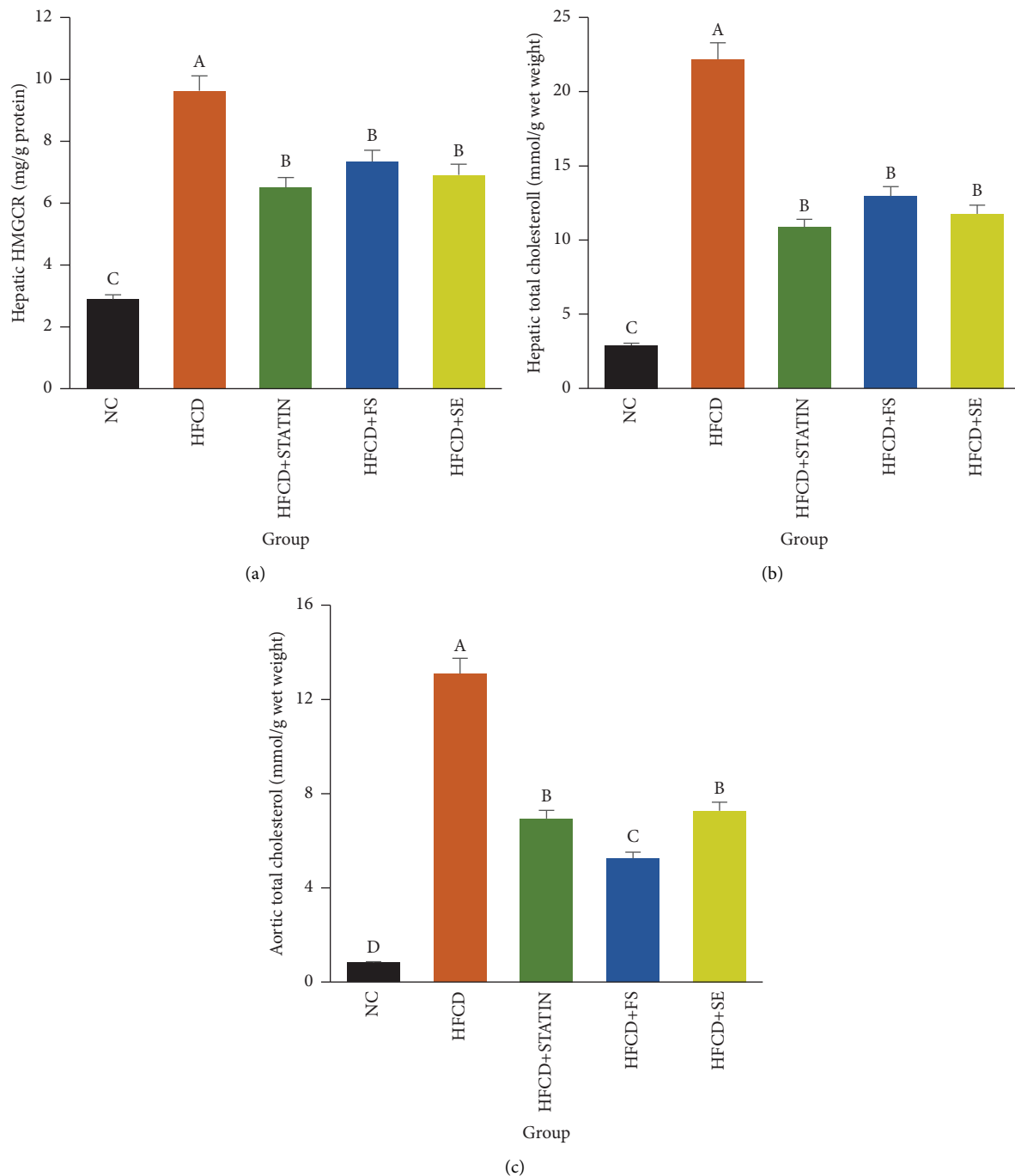


FIGURE 5: Effects of EBN on (a) hepatic HMGCR, (b) hepatic total cholesterol, and (c) aortic total cholesterol in hypercholesterolemic rabbits. Values shown are expressed as the mean \pm standard error of the mean (SEM, $n = 5$). Different letters mean significant differences between groups ($p < 0.05$, $a > b > c > d$). NC: normal control; HFCD: high-fat high-cholesterol diet; STATIN: simvastatin; FS: full stew of EBN; SE: stew extract of EBN.

expression by 1.7-fold and 1.4-fold was observed in the liver and aorta of the HFCD group, respectively. EBN and simvastatin interventions significantly enhanced mRNA expression levels of these genes in both liver (ABCA1: HFCD + STATIN > HFCD + SE > HFCD + FS; LCAT: HFCD + STATIN > HFCD + FS > HFCD + SE) and aorta (ABCA1: HFCD + FS > HFCD + STATIN > HFCD + SE; LCAT: HFCD + FS > HFCD + STATIN > HFCD + SE) of

hypercholesterolemic rabbits ($p < 0.05$). The primary function of ABCA1 is to transfer intracellular free cholesterol and phospholipids to extracellular lipid-poor apolipoprotein (mainly ApoAI), where they are assembled to form nascent HDL [44]. Meanwhile, LCAT has the ability to transform free cholesterol in nascent HDL into cholesterol ester (CE), which can then be converted into mature HDL as well as blocking cholesterol export from HDL [45].

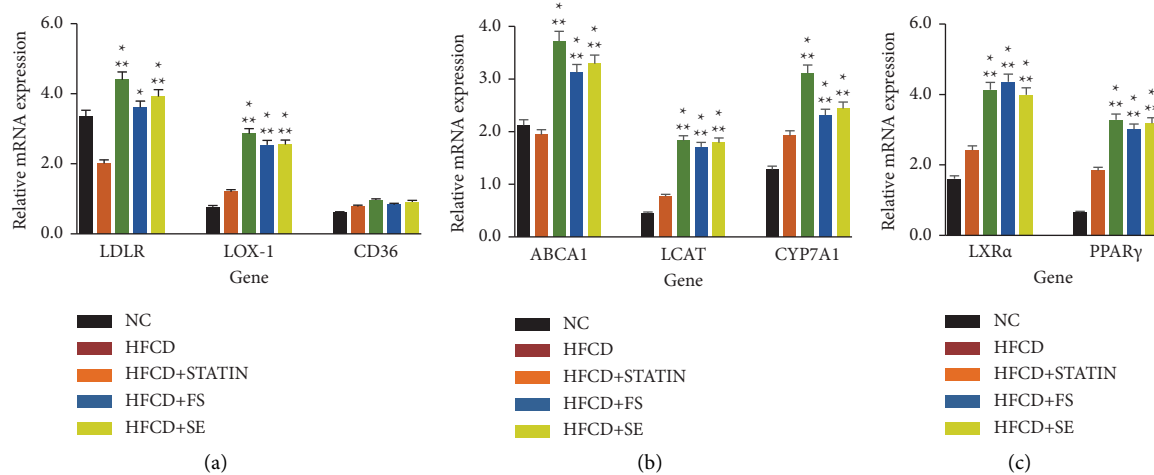


FIGURE 6: Gene expressions in the liver tissue of experimental rabbits after 12 weeks of dietary intervention. Modulation of hepatic mRNA expression by EBN on key genes involved in (a) receptor-mediated uptake of cholesterol, (b) cholesterol efflux, and (c) cholesterol-sensing signaling. Values shown are expressed as the mean \pm standard error of the mean (SEM, $n = 5$). * $p < 0.05$ compared to the HFCD group and ** $p < 0.05$ compared to the NC group. NC: normal control; HFCD: high-fat high-cholesterol diet; STATIN: simvastatin; FS: full stew of EBN; SE: stew extract of EBN.

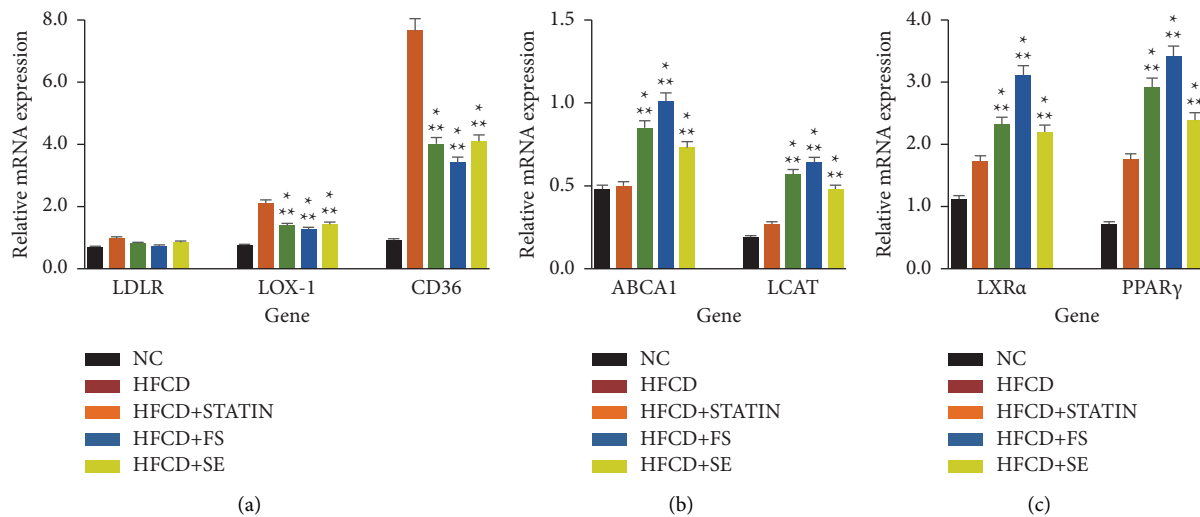


FIGURE 7: Gene expressions in the aorta tissue of experimental rabbits after 12 weeks of dietary intervention. Modulation of aortic mRNA expression by EBN on key genes involved in (a) receptor-mediated uptake of cholesterol, (b) cholesterol efflux, and (c) cholesterol-sensing signaling. Values shown are expressed as the mean \pm standard error of the mean (SEM, $n = 5$). * $p < 0.05$ compared to the HFCD group and ** $p < 0.05$ compared to the NC group. NC: normal control; HFCD: high-fat high-cholesterol diet; STATIN: simvastatin; FS: full stew of EBN; SE: stew extract of EBN.

From the transcriptional analyses, ABCA1 and LCAT genes were highly expressed in the liver as compared to the aorta of experimental rabbits. Moreover, in mice with liver-specific ABCA1 deletion, HDL levels decreased by over 80%, indicating that the liver is the principal source of HDL in the blood [46]. The modulation of the hepatic ABCA1 and LCAT expressions could be the major contributor to the augmentation of serum HDL-c levels. EBN and simvastatin enhanced reverse cholesterol transport (RCT) by upregulating ABCA1 and LCAT genes, thereby reducing cholesterol accumulation in the

liver and aorta. RCT plays a significant role in atherogenesis as HDL-c transfers excess cholesterol from peripheral tissues to the liver for excretion [46, 47].

CYP7A1 is a critical rate-limiting enzyme in cholesterol-to-bile acid conversion. The production of bile acids, which are the last products of cholesterol catabolism, and their excretion into the feces help reduce the amount of excess cholesterol in the liver [8]. Therefore, the modulation of specific hepatic CYP7A1 in the hypercholesterolemic model of this study was identified to evaluate the potential of EBN in enhancing the hepatic cholesterol elimination. Figure 6(b) shows that the hepatic mRNA

expression of the CYP7A1 level was significantly increased in the hypercholesterolemic rabbits in the following order: HCFD > HCFD + FS > HCFD + SE > HCFD + STATIN as compared to the normal group ($p < 0.05$). EBN and simvastatin enhanced the cholesterol excretion in the liver of hypercholesterolemic rabbits by upregulating the hepatic CYP7A1 expression (HCFD + FS: 1.2-fold; HCFD + SE: 1.3-fold; HCFD + STATIN: 2.4-fold). Meanwhile, an increase in the hepatic CYP7A1 gene transcription in hypercholesterolemic rabbits in the HCFD group may have been a compensatory response to hepatic cholesterol accumulation [48]. The enhancement of RCT following EBN and simvastatin intervention reduced cholesterol burden and lipotoxicity as well as prevented hepatosteatosis occurrence in hypercholesterolemic rabbits.

EBN modulates cholesterol influx and efflux in both the liver and aorta, which is in accordance with the results of the hepatic and aortic TC in this study. Increased oxLDL uptake and/or decreased cholesterol efflux result in esterified cholesterol deposition in macrophage cytoplasm and the formation of foam cells [49]. In addition, the severity of atherosclerosis lesions in cholesterol-fed rabbits has also been associated with the cholesterol content of the aorta [50]. In accordance with the total cholesterol levels in tissues measured in this study, tunica intima thickness of the aorta was highly related to the TC levels (liver: $r = 0.904$; aorta: $r = 0.913$; $p < 0.05$). The improved serum lipid profile and tissue TC by EBN attenuate hepatic steatosis and atheromatous plaque formation in hypercholesterolemic rabbits.

The administration of the HFC diet significantly altered cholesterol-sensing signaling genes by increasing the expression of nuclear receptors LXR α and PPAR γ in both liver (Figure 6(c)) and the aorta (Fig. 7(c)) of the HCFD group, as compared to the NC group ($p < 0.05$). In comparison to the HCFD group, EBN supplementation significantly enhanced ($p < 0.05$) the mRNA expression of hepatic LXR α (HCFD + FS: 1.8-fold; HCFD + SE: 1.6-fold) and PPAR γ (HCFD + FS: 1.6-fold; HCFD + SE: 1.7-fold) in the hypercholesterolemic rabbits. The modulatory effects of EBN on LXR α /PPAR γ activation were comparable to simvastatin treatment in the liver ($p > 0.05$). A similar alteration pattern of these genes was observed in aortic LXR α and PPAR γ (HCFD + FS > HCFD + SE; $p < 0.05$).

PPAR γ is a transcription factor that belongs to the nuclear receptor superfamily that regulates the macrophage cholesterol efflux by stimulating the expression of LXR α [6]. The activation of LXR α stimulates the expression of ABCA1 and CYP7A1, thus promoting RCT by increasing the HDL-c production, bile acid biogenesis, and cholesterol excretion [51]. Meanwhile, the suppression of hepatic ABCA1 and CYP7A1 has accelerated aortic cholesterol accumulation in LXR α -deficient mice, indicating that both ABCA1 protein and CYP7A1 enzyme activity are LXR α -dependent [52, 53]. In fact, the suppression of LXR α /PPAR γ activation also downregulates ABCA1, LDLR, and HMGCR expressions in mice fed with the HFC diet [54]. Therefore, the activation of the PPAR γ /LXR α signaling pathway by EBN provides a significant role in the modulation of cholesterol homeostasis in both the liver and the aorta tissues.

It can be suggested that the bioactive compounds in EBN may produce a favorable effect on cholesterol metabolism and atherosclerotic plaque stabilization. As an important metabolite in EBN, sialic acid was proven to improve cholesterol metabolism by upregulating LDLR via the suppression of HMGCR gene expression in HepG2 cell lines [10]. Furthermore, a recent report by Kawanishi et al. [55] showed that the aortic atherosclerotic plaque development and lipid deposition in the liver were reduced by 18.9% and 26.7%, respectively, in HFD-fed ApoE knockout mice supplemented with sialic acid. According to Hou et al. [56], the incorporation of sialic acid into drinking water improved intracellular cholesterol transfer to plasma (42.9%), cholesterol transported to the liver for excretion (35.8%), and cholesterol excreted in the feces (50.4%) in mice fed high-fat diet enriched with 1% cholesterol. However, the authors have claimed that this exogenous supplementation of sialic acid did not show any changes in ABCA1 and CYP7A1 expressions, suggesting that the presence of other bioactive in EBN may result in the alteration of these RCT-related genes.

The hypocholesterolemic effects of EBN in the liver were executed via four major mechanisms: increasing the clearance of circulating LDL-c and oxLDL in the blood through upregulation of the LDLR and LOX-1 genes, prevention of cholesterol synthesis by lowering the activity of the hepatic HMGCR enzyme, promoting hepatic cholesterol balance via upregulation of hepatic ABCA1 and LCAT genes which are activated by PPAR γ /LXR α signaling, and increasing the removal of excess hepatic cholesterol through cholesterol-to-bile acid conversion via upregulation of the hepatic CYP7A1 gene. Given the potential of FS and SE to suppress cholesterol synthesis while also expressing hepatic LDLR activity, EBN may prove to be effective as a cholesterol-lowering agent.

As EBN regulates hepatic cholesterol metabolism, the reduction in atheromatous plaque formation was attained. The activation of PPAR γ /LXR α initiates a negative feedback loop to inhibit the intake of additional cholesterol as foam cells become overloaded with cholesterol. Findings from this study demonstrated the modulatory effects of EBN on aortic cholesterol metabolism through two major mechanisms as follows: (1) controlled cholesterol uptake by downregulation of aortic LOX-1 and CD36 expression and (2) increased cholesterol efflux through RCT mechanism via upregulating aortic ABCA1 and LCAT genes which were activated by PPAR γ /LXR α signaling. Given these findings, the fact that the HFC diet increases CD36 and ABCA1 expressions in the aorta may provide useful information for understanding the mechanism underlying the influence of dietary cholesterol on atherosclerotic plaque formation.

The regulation of cholesterol metabolism is not only activated by PPAR γ alone, but it could be triggered by other peroxisome proliferator-activated receptors (PPARs) such as PPAR α and PPAR β/δ . The activation of PPAR α by fibrates consistently showed positive effects on plasma levels of HDL-c and decreased levels of "atherogenic lipids," such as triglycerides and LDL-c [57]. In fact, the expression of the CYP7A1 gene in the liver tissue was suppressed by

ciprofibrate, a PPAR α agonist [58]. The action of PPAR β/δ agonists was found to exhibit similar effects as PPAR α and PPAR γ agonists, by increasing the plasma level of HDL-c and decreasing the plasma level of LDL-c. Different rodent and primate models have supported these beneficial benefits [59–61]. In addition, it has been demonstrated that PPAR β/δ decreases cholesterol absorption and enhances transintestinal cholesterol efflux in the intestine [62]. In cholesterol-sensing signaling, PPARs in conjunction with other nuclear receptors such as LXR are vital for balancing cholesterol metabolism homeostasis.

4. Conclusion

The efficacy of FS of EBN in ameliorating hypercholesterolemia and atherosclerosis is on par with simvastatin drugs as compared to SE, suggesting that the combination of both soluble and insoluble fractions of EBN produced better effects on cholesterol homeostasis than soluble fractions alone. These findings narrate the use of EBN as a new therapeutic approach targeting cholesterol flux in the liver and aorta. In fact, EBN potentially alleviates the severity of NAFLD by reducing hepatic steatosis caused by hypercholesterolemia. The effects of EBN on improving serum lipid profiles and stabilizing atherosclerotic plaque in hypercholesterolemic rabbits suggested that EBN may represent a promising candidate for a therapeutic agent for the treatment or prevention of atherosclerosis.

Data Availability

The biochemical, histology, and gene expression data used to support the findings of this study are included within the article.

Additional Points

Highlights. (i) EBN significantly improved lipid and coagulation profiles of hypercholesterolemic rabbits. (ii) EBN significantly reduced hepatosteatosis and stabilized atherosclerotic plaque formation in hypercholesterolemic rabbits. (iii) EBN significantly induced genes related to cholesterol uptake (LDLR, LOX-1, and CD36), cholesterol efflux (ABCA1, LCAT, and CYP7A1), and cholesterol-sensing signaling (LXR α and PPAR γ). (iv) EBN supplementation could be an effective food product for the treatment or prevention of atherosclerosis by regulating cholesterol metabolism.

Disclosure

The funders had no role in the design of the study; in the collection, analyses, or interpretation of data; in the writing of the manuscript, or in the decision to publish the results.

Conflicts of Interest

The authors declare that they have no conflicts of interest.

Authors' Contributions

N.N.M.N. and R.M.I. conceptualized the study. N.N.M.N. and R.M.I. proposed the methodology. N.N.M.N., R.M.I., and N.I. provided the software. N.N.M.N. and R.M.I. validated the study. N.N.M.N., R.M.I., N.I., and C.K.W. performed the formal analysis. N.N.M.N. and R.M.I. investigated the data. R.M., M.Z.A.B., and N.A.A.R. collected the resources. N.N.M.N., R.M.I., N.I., and C.K.W. curated the data. N.N.M.N. wrote the manuscript. M.Z.A.B. reviewed and edited the study. N.N.M.N. and R.M.I. visualized the study. M.Z.A.B., R.M., and N.A.A.R. supervised the study. M.Z.A.B., R.M., and N.A.A.R. administered the project. M.Z.A.B. acquired the funding. All authors critically proofread the manuscript, agreed, and approved for publication.

Acknowledgments

The authors are thankful to the Natural Medicine and Products Research Laboratory (Institute of Bioscience), Universiti Putra Malaysia (UPM), Faculty of Veterinary Medicine (UPM), and Faculty of Medicine and Health Sciences (UPM) for providing infrastructures and technical support for the analysis performed. The authors are grateful for the financial support from the Research Management Centre of UPM under the Putra Grant-Putra Young Initiative (IPM) (Grant no. 9543900).

References

- [1] J. Borén, M. J. Chapman, R. M. Krauss et al., "Low-density lipoproteins cause atherosclerotic cardiovascular disease: pathophysiological, genetic, and therapeutic insights: a consensus statement from the European Atherosclerosis Society Consensus Panel," *European Heart Journal*, vol. 41, no. 24, pp. 2313–2330, 2020.
- [2] L. Trapani, M. Segatto, and V. Pallottini, "Regulation and deregulation of cholesterol homeostasis: the liver as a metabolic power station," *World Journal of Hepatology*, vol. 4, no. 6, p. 184, 2012.
- [3] J. Fan, L. Liu, Q. Liu et al., "CKIP-1 limits foam cell formation and inhibits atherosclerosis by promoting degradation of Oct-1 by REG γ ," *Nature Communications*, vol. 10, no. 1, p. 425, 2019.
- [4] A. Arjuman and N. C. Chandra, "LOX-1: a potential target for therapy in atherosclerosis; an in vitro study," *The International Journal of Biochemistry and Cell Biology*, vol. 91, pp. 65–80, 2017.
- [5] S.-J. Jeong, M.-N. Lee, and G. T. Oh, "The role of macrophage lipophagy in reverse cholesterol transport," *Endocrinology and Metabolism*, vol. 32, no. 1, p. 41, 2017.
- [6] P. Xu, Y. Zhai, and J. Wang, "The role of PPAR and its cross-talk with CAR and LXR in obesity and atherosclerosis," *International Journal of Molecular Sciences*, vol. 19, no. 4, p. 1260, 2018.
- [7] A. Volobueva, D. Zhang, A. V. Grechko, and A. N. Orekhov, "Foam cell formation and cholesterol trafficking and metabolism disturbances in atherosclerosis," *Cor et Vasa*, vol. 61, no. 1, pp. 48–55, 2019.
- [8] J. Y. L. Chiang and J. M. Ferrell, "Up to date on cholesterol 7 alpha-hydroxylase (CYP7A1) in bile acid synthesis," *Liver Research*, vol. 4, no. 2, pp. 47–63, 2020.

- [9] N. C. Ward, G. F. Watts, and R. H. Eckel, "Statin toxicity," *Circulation Research*, vol. 124, no. 2, pp. 328–350, 2019.
- [10] M. N. Akmal, I.-S. Abdul Razak, R. Mansor et al., "High-dose edible bird's nest extract (ebn) upregulates ldl-r via suppression of hmgr gene expression in hepg2 cell lines," *Sains Malaysiana*, vol. 49, no. 10, pp. 2433–2442, 2020.
- [11] Z. Yida, M. U. Imam, M. Ismail et al., "Edible bird's nest prevents high fat diet-induced insulin resistance in rats," *Journal of Diabetes Research*, vol. 2015, Article ID 760535, 11 pages, 2015a.
- [12] Z. Yida, M. U. Imam, M. Ismail, N. Ismail, and Z. Hou, "Edible bird's nest attenuates procoagulation effects of high-fat diet in rats," *Drug Design, Development and Therapy*, vol. 9, pp. 3951–3959, 2015.
- [13] N. N. Mohamad Nasir, R. Mohamad Ibrahim, M. Z. Abu Bakar, R. Mahmud, and N. A. Ab Razak, "Characterization and extraction influence protein profiling of edible bird's nest," *Foods*, vol. 10, no. 10, p. 2248, 2021.
- [14] J. W. Shin, I. C. Seol, and C. G. Son, "Interpretation of animal dose and human equivalent dose for drug development," *The Journal of Korean Oriental Medicine*, vol. 31, 2010.
- [15] R. Sujatha and S. Kavitha, "Atherogenic indices in stroke patients: a retrospective study," *Iran J Neurol*, vol. 16, no. 2, pp. 78–82, 2017.
- [16] M. J. Andrés-Manzano, V. Andrés, and B. Dorado, "Oil red o and hematoxylin and eosin staining for quantification of atherosclerosis burden in mouse aorta and aortic root," *Methods in Molecular Biology*, vol. 1339, pp. 85–99, 2015.
- [17] R. Mohamad Ibrahim, N. N. Mohamad Nasir, M. Z. Abu Bakar, R. Mahmud, and N. A. Ab Razak, "The authentication and grading of edible bird's nest by metabolite, nutritional, and mineral profiling," *Foods*, vol. 10, no. 7, p. 1574, 2021.
- [18] G. Alarcon, J. Roco, M. Medina, A. Medina, M. Peral, and S. Jerez, "High fat diet-induced metabolically obese and normal weight rabbit model shows early vascular dysfunction: mechanisms involved," *International Journal of Obesity*, vol. 42, no. 9, pp. 1535–1543, 2018.
- [19] A. A. Adeneye, O. O. Adeyemi, and E. O. Agbaje, "Anti-obesity and antihyperlipidaemic effect of *Hunteria umbellata* seed extract in experimental hyperlipidaemia," *Journal of Ethnopharmacology*, vol. 130, no. 2, pp. 307–314, 2010.
- [20] Z. Yida, M. U. Imam, M. Ismail et al., "N-acetylneuraminic acid supplementation prevents high fat diet-induced insulin resistance in rats through transcriptional and nontranscriptional mechanisms," *BioMed Research International*, vol. 2015, Article ID 602313, 10 pages, 2015b.
- [21] M. Nakata, D. Gantulga, P. Santoso et al., "Paraventricular NUCB2/Nesfatin-1 supports oxytocin and vasopressin neurons to control feeding behavior and fluid balance in male mice," *Endocrinology*, vol. 157, no. 6, pp. 2322–2332, 2016.
- [22] L. Bozzetto, G. Costabile, G. Della Pepa et al., "Dietary fibre as a unifying remedy for the whole spectrum of obesity-associated cardiovascular risk," *Nutrients*, vol. 10, no. 7, p. 943, 2018.
- [23] Z. Hou, P. He, M. U. Imam et al., "Edible bird's nest prevents menopause-related memory and cognitive decline in rats via increased hippocampal sirtuin-1 expression," *Oxidative Medicine and Cellular Longevity*, vol. 2017, Article ID 7205082, 8 pages, 2017.
- [24] M. Olamoyegun, R. Oluyombo, and S. Asaolu, "Evaluation of dyslipidemia, lipid ratios, and atherogenic index as cardiovascular risk factors among semi-urban dwellers in Nigeria," *Annals of African Medicine*, vol. 15, no. 4, p. 194, 2016.
- [25] S. Bhardwaj, J. Bhattarjee, M. K. Bhatnagar, and S. Tyagi, "Atherogenic index of plasma, castelli risk index and atherogenic coefficient new parameters in assessing cardiovascular risk," *International Journal of Pharmacy and Biological Sciences*, vol. 3, pp. 359–364, 2013.
- [26] M. N. Akmal, A. R. Intan-Shameha, M. Ajat, R. Mansor, A. B. Z. Zuki, and A. Ideris, "Edible bird's nest (EBN) supplementation ameliorates the progression of hepatic changes and atherosclerosis in hypercholesterolaemic-induced rats," *Malaysian Journal of Microscopy*, vol. 14, pp. 103–114, 2018.
- [27] N. A. Ashry, R. R. Abdelaziz, G. M. Suddek, and M. A. Saleh, "Canagliflozin ameliorates aortic and hepatic dysfunction in dietary-induced hypercholesterolemia in the rabbit," *Life Sciences*, vol. 280, Article ID 119731, 2021.
- [28] K. Hosoyamada, H. Uto, Y. Imamura et al., "Fatty liver in men is associated with high serum levels of small, dense low-density lipoprotein cholesterol," *Diabetology and Metabolic Syndrome*, vol. 4, no. 1, p. 34, 2012.
- [29] S. Guo, H. Tian, R. Dong et al., "Exogenous supplement of N-acetylneuraminic acid ameliorates atherosclerosis in apolipoprotein E-deficient mice," *Atherosclerosis*, vol. 251, pp. 183–191, 2016.
- [30] Y. Yin, Z. Li, L. Gao, Y. Li, J. Zhao, and W. Zhang, "AMPK-dependent modulation of hepatic lipid metabolism by nesfatin-1," *Molecular and Cellular Endocrinology*, vol. 417, pp. 20–26, 2015.
- [31] M.-H. Gwon, Y.-S. Im, A.-R. Seo, K. Y. Kim, H.-R. Moon, and J.-M. Yun, "Phenethyl isothiocyanate protects against high fat/cholesterol diet-induced obesity and atherosclerosis in c57bl/6 mice," *Nutrients*, vol. 12, no. 12, p. 3657, 2020.
- [32] B. B. Misra, S. R. Puppala, A. G. Comuzzie, M. C. Mahaney, J. L. VandeBerg, and M. Olivier, "Analysis of serum changes in response to a high fat high cholesterol diet challenge reveals metabolic biomarkers of atherosclerosis," *PLoS One*, vol. 14, no. 4, Article ID e0214487, 2019.
- [33] A. A. Rehman, A. Riaz, M. A. Asghar, M. L. Raza, S. Ahmed, and K. Khan, "In vivo assessment of anticoagulant and antiplatelet effects of *Syzygium cumini* leaves extract in rabbits," *BMC Complementary and Alternative Medicine*, vol. 19, no. 1, p. 236, 2019.
- [34] Z. Yida, M. U. Imam, M. Ismail et al., "N-acetylneuraminic acid attenuates hypercoagulation on high fat diet-induced hyperlipidemic rats," *Food and Nutrition Research*, vol. 59, no. 1, Article ID 29046, 2015c.
- [35] R. T. Almaraz, Y. Tian, R. Bhattacharya, E. Tan, S. H. Chen, and M. R. Dallas, "Metabolic flux increases glycoprotein sialylation: implications for cell adhesion and cancer metastasis," *Molecular and Cellular Proteomics*, vol. 11, no. 7, pp. M112.017558-1–M112.017558-12, 2012.
- [36] J. I. Borissoff, S. Heeneman, E. Kiliç et al., "Early atherosclerosis exhibits an enhanced procoagulant state," *Circulation*, vol. 122, no. 8, pp. 821–830, 2010.
- [37] K. E. Kryczka, M. Kruk, M. Demkow, and B. Lubiszewska, "Fibrinogen and a triad of thrombosis, inflammation, and the renin-angiotensin system in premature coronary artery disease in women: a new insight into sex-related differences in the pathogenesis of the disease," *Biomolecules*, vol. 11, no. 7, p. 1036, 2021.
- [38] S. Surma and M. Banach, "Fibrinogen and atherosclerotic cardiovascular diseases—review of the literature and clinical studies," *International Journal of Molecular Sciences*, vol. 23, no. 1, p. 193, 2021.
- [39] F. Xu, H. Yu, C. Lu, J. Chen, and W. Gu, "The cholesterol-lowering effect of alisol acetates based on hm-g-coa reductase and its molecular mechanism," *Evidence-based Complementary and Alternative Medicine*, vol. 2016, Article ID 4753852, 11 pages, 2016.

- [40] S. Wang, B. Miller, N. R. Matthan et al., "Aortic cholesterol accumulation correlates with systemic inflammation but not hepatic and gonadal adipose tissue inflammation in low-density lipoprotein receptor null mice," *Nutrition Research*, vol. 33, no. 12, pp. 1072–1082, 2013.
- [41] H.-J. Park, U. J. Jung, M.-K. Lee et al., "Modulation of lipid metabolism by polyphenol-rich grape skin extract improves liver steatosis and adiposity in high fat fed mice," *Molecular Nutrition and Food Research*, vol. 57, no. 2, pp. 360–364, 2012.
- [42] Y. Zhao, Y. Yang, R. Xing et al., "Hyperlipidemia induces typical atherosclerosis development in Ldlr and Apoe deficient rats," *Atherosclerosis*, vol. 271, pp. 26–35, 2018.
- [43] D. F. Schaeffer, M. Riaz, and K. S. Parhar, "LOX-1 augments oxLDL uptake by lysoPC-stimulated murine macrophages but is not required for oxLDL clearance from plasma," *Journal of Lipid Research*, vol. 50, no. 8, pp. 1676–1684, 2009.
- [44] S. Wang and J. D. Smith, "ABCA1 and nascent HDL biogenesis," *BioFactors*, vol. 40, no. 6, pp. 547–554, 2014.
- [45] S. Lee, M.-S. Lee, E. Chang et al., "Mulberry fruit extract promotes serum HDL-cholesterol levels and suppresses hepatic microRNA-33 expression in rats fed high cholesterol/cholic acid diet," *Nutrients*, vol. 12, no. 5, p. 1499, 2020.
- [46] L. R. Brunham and M. R. Hayden, "Human genetics of HDL: insight into particle metabolism and function," *Progress in Lipid Research*, vol. 58, pp. 14–25, 2015.
- [47] Q. Jia, H. Cao, D. Shen et al., "Quercetin protects against atherosclerosis by regulating the expression of PCSK9, CD36, PPAR γ , LXRA and ABCA1," *International Journal of Molecular Medicine*, vol. 44, no. 3, pp. 893–902, 2019.
- [48] K. W. Chan, M. Ismail, N. Mohd Esa, M. U. Imam, D. J. Ooi, and N. M. H. Khong, "Dietary supplementation of defatted kenaf (*Hibiscus cannabinus* L.) seed meal and its phenolics-saponins rich extract effectively attenuates diet-induced hypercholesterolemia in rats," *Food and Function*, vol. 9, no. 2, pp. 925–936, 2018.
- [49] X. H. Yu, Y. C. Fu, D. W. Zhang, K. Yin, and C. K. Tang, "Foam cells in atherosclerosis," *Clinica Chimica Acta*, vol. 424, pp. 245–252, 2013.
- [50] M. Ibrahim, I. A. Ahmed, M. A. Mikail et al., "Baccaurea angulata fruit juice reduces atherosclerotic lesions in diet-induced Hypercholesterolemic rabbits," *Lipids in Health and Disease*, vol. 16, no. 1, p. 134, 2017.
- [51] T. Sozański, A. Z. Kucharska, A. Szumny et al., "The protective effect of the *Cornus mas* fruits (cornelian cherry) on hypertriglyceridemia and atherosclerosis through PPAR α activation in hypercholesterolemic rabbits," *Phytomedicine*, vol. 21, no. 13, pp. 1774–1784, 2014.
- [52] D. A. Chistiakov, Y. V. Bobryshev, and A. N. Orekhov, "Macrophage-mediated cholesterol handling in atherosclerosis," *Journal of Cellular and Molecular Medicine*, vol. 20, no. 1, pp. 17–28, 2015.
- [53] Y.-W. Hu, L. Zheng, and Q. Wang, "Regulation of cholesterol homeostasis by liver X receptors," *Clinica Chimica Acta*, vol. 411, no. 9–10, pp. 617–625, 2010.
- [54] Y.-W. Hu, X. Ma, J.-L. Huang et al., "Dihydrocapsaicin attenuates plaque formation through a ppar γ /lxra pathway in apoE $^{-/-}$ mice fed a high-fat/high-cholesterol diet," *PLoS One*, vol. 8, no. 6, Article ID e66876, 2013.
- [55] K. Kawanishi, J. K. Coker, K. V. Grunddal et al., "Dietary Neu5Ac intervention protects against atherosclerosis associated with human-like Neu5Gc loss—brief report," *Arteriosclerosis, Thrombosis, and Vascular Biology*, vol. 41, no. 11, pp. 2730–2739, 2021.
- [56] P. Hou, S. Hu, J. Wang et al., "Exogenous supplement of N-acetylneuraminic acid improves macrophage reverse cholesterol transport in apolipoprotein E-deficient mice," *Lipids in Health and Disease*, vol. 18, no. 1, p. 24, 2019.
- [57] F. Hong, S. Pan, Y. Guo, P. Xu, and Y. Zhai, "PPARs as nuclear receptors for nutrient and energy metabolism," *Molecules*, vol. 24, no. 14, p. 2545, 2019.
- [58] M. Marrapodi and J. Y. L. Chiang, "Peroxisome proliferator-activated receptor α (PPAR α) and agonist inhibit cholesterol 7 α -hydroxylase gene (CYP7A1) transcription," *Journal of Lipid Research*, vol. 41, no. 4, pp. 514–520, 2000.
- [59] E. J. Olson, G. L. Pearce, N. P. Jones, and D. L. Sprecher, "Lipid effects of peroxisome proliferator-activated receptor- Δ agonist GW501516 in subjects with low high-density lipoprotein cholesterol," *Arteriosclerosis, Thrombosis, and Vascular Biology*, vol. 32, no. 9, pp. 2289–2294, 2012.
- [60] H. E. Bays, S. Schwartz, T. Littlejohn et al., "MBX-8025, A novel peroxisome proliferator receptor- δ agonist: lipid and other metabolic effects in dyslipidemic overweight patients treated with and without atorvastatin," *Journal of Clinical Endocrinology and Metabolism*, vol. 96, no. 9, pp. 2889–2897, 2011.
- [61] W. R. Oliver, J. L. Shenk, M. R. Snaithe et al., "A selective peroxisome proliferator-activated receptor agonist promotes reverse cholesterol transport," *Proceedings of the National Academy of Sciences*, vol. 98, no. 9, pp. 5306–5311, 2001.
- [62] C. L. Vrins, A. E. van der Velde, K. van den Oever et al., "Peroxisome proliferator-activated receptor delta activation leads to increased transintestinal cholesterol efflux," *Journal of Lipid Research*, vol. 50, no. 10, pp. 2046–2054, 2009.